Article

Journal of
Nanoscience and Nanotechnology
Vol. 16, 1–10, 2016
www.aspbs.com/jnn

Graphene Oxide Induces Toxicity and Alters Energy Metabolism and Gene Expression in *Ralstonia Solanacearum*

Juanni Chen[1], Shili Li[1], Jinxiang Luo[1], Yongqiang Zhang[1], and Wei Ding[1, 2, *]

[1] *Laboratory of Natural Product Pesticide, College of Plant Protection, Southwest University, Chongqing, 400715, P. R. China*
[2] *Tobacco Scientific Research Institute of Chongqing, Chongqing, 400715, P. R. China*

Graphene oxide (GO) is a promising material for development as an antibacterial, phytoprotective agent due to its contact-based antibacterial activity induced by its physical and chemical properties. However, the mechanism underlying the antibacterial effect of GO has yet to be elucidated. In the current study, we investigated the effects of GO on the phytopathogen *R. solanacearum* at the molecular level with a specific focus on energy metabolism. Under controlled conditions, the bacteriostatic and bactericidal actions of GO were investigated with respect to concentration, treatment time and rotation speed. Transmission electron microscopy (TEM) and destabilization assays revealed that GO caused injury to bacterial cell membrane structures. Furthermore, adenosine triphosphate (ATP) levels decreased after exposure to sheets of GO, while malondialdehyde levels significantly increased, indicating the occurrence of lipid oxidation. A series of genes related to bacterial virulence, motility and oxidative stress were selected to evaluate the molecular mechanism underlying GO's effects on *R. solanacearum*. Using quantitative reverse transcription polymerase chain reaction (RT-qPCR), we showed that in the presence of GO, the expression levels of genes involved in virulence and motility were down regulated, with the exception of *popA*. The *phcA*, *hrpB* and *flgG* genes were significantly downregulated by 2.61-, 3.45- and 4.22-fold, respectively. Conversely, the expression levels of *sodB*, *oxyR* and *dps*, three important oxidative stress genes, were upregulated by 1.82-, 2.17-, and 3.79-fold, respectively. These findings confirmed that cell membrane damage and oxidative stress were responsible for the antibacterial actions of GO, in addition to disturbances to energy metabolism processes.

Keywords:

1. INTRODUCTION

Research efforts in nanoscience and nanotechnology have led to the ability to produce materials and devices in the nanometer range, which hold significant promise for all aspects of agriculture, especially in the development of novel solutions to provide protection and nutrition to plants.[1] Recently, nanomaterials have been widely applied to achieve controlled release of fertilizer and micronutrients, pesticide degradation, biopesticide stabilization, plant pathogen and pesticide detection, and soil conservation and remediation.[1, 2] Most notably, several synthetic nanomaterials, including inorganic, organic, and metallic materials, have attracted increasing attention for use in applications to inactivate phytopathogenic bacteria and fungi.[1]

Graphene oxide (GO), a material that can be made into a single-atom-thick, two-dimensional sheet of hexagonally arranged carbon, has attracted tremendous scientific interest in recent decades because of its unique properties, including its tensile strength, high surface area and thermal conductivity.[3, 4] While the physical and chemical properties of GO may be attractive for a variety of applications, they have also led to concerns about GO's possible adverse effects on both bacterial and mammalian cells.[4–6] In 2010, Fan et al. conducted a study on the antibacterial activities of GO;[6] since then, GO and its derivatives have been extensively studied as promising candidate antibacterial agents. A number of publications have reported the

*Author to whom correspondence should be addressed.

potential application of GO in antimicrobial products.[7] As previously reviewed by Liu et al., a comparative study of our graphene-based nanoparticles, including GO and reduced graphene oxide (rGO) dispersions, showed that GO possesses a wide range of antibacterial activity towards both Gram-positive and Gram-negative bacteria, including against food-borne *Escherichia coli* and *Staphylococcus aureus*.[6, 8] Another investigation showed that rGO nanowalls exhibited a high degree of antibacterial activity, which was attributed to enhanced charge transfer between the nanowalls and bacteria and to the sharp edges of the nanowalls coming into contact with bacteria.[9]

The above-detailed merits of GO have prompted its exploitation in the management of plant diseases and as a new type of antibacterial agent to control phytopathogens. Previous studies have demonstrated that GO possesses strong bactericidal activity and can induce the death of the phytopathogens *Xanthomonas oryzae* pv. *oryzae* (*Xoo*),[10] *Pseudomonas syringae* (*P. syringae*), and *Xanthomonas campestris* pv. *undulosa* (*X. campestris*)[11] and the fungus *Fusarium graminearum* (*F. graminearum*).[11] However, little information is available regarding the effects of GO on *R. solanacearum*, anon-spore-forming, rod-shaped, devastating Gram-negative pathogenic bacterium that induces bacterial wilt disease.[12] This pathogen has a broad geographic distribution and wide host range, and it is endemic in most subtropical and tropical regions of the world.[13] *R. solanacearum* has the ability to colonize host plants and cause yellow-brown discoloration of vascular tissue, which progresses into the formation of black streaks.[14] Traditionally, chemical pesticides and agricultural practice shave been used to manage the disease;[15] however, there remains a need for novel, highly efficient strategies of adequately controlling these bacteria. Before considering the potential of using GO as an antibacterial agent against *R. solanacearum*, it is necessary to thoroughly understand its antibacterial mechanisms.

Mechanical injury and oxidative stress are considered the major contributors of GO cytotoxicity.[8, 10, 16] We recently demonstrated that GO produced powerful cytotoxic effects when used as a treatment against plant bacterial and fungal conidia.[11] Several studies have also proposed that GO damages bacterial cell membranes when its extremely sharp edges come into contact with bacteria, which was shown to be an effective mechanism of bacterial inactivation.[17] Additionally, the enhanced electrical properties (i.e., charge transfer) of graphene nanoparticles have been reported to induce the production of reactive oxygen species (ROS), primarily including hydroxyl radicals, H_2O_2 and single oxygen (O^{-2}), which are thought to be responsible for the high antibacterial activity of graphene.[18] However, the effects of GO on bacterial energy metabolism and the molecular mechanisms underlying its antibacterial activity toward *R. solanacearum* are still largely unexplored.

All life activity depends on constant energy production and transduction. The bacterial cytoplasmic membrane is vital for solute/nutrient cell import, ATP synthesis and cell motility. Most importantly, ion gradients formed across the cell membrane act as aproton motive force to drive a variety of metabolic processes. In the current study, to clarify GO's influence on energy-transducing processes and metabolism in bacteria and gain a comprehensive understanding of its high antibacterial activity at a molecular level, we examined its antibacterial activity against *R. solanacearum* by investigating its effects on ATP production, lipid peroxidation, membrane sensitivity using quantitative reverse transcription polymerase chain reaction (RT-qPCR).

2. MATERIALS AND METHODS

2.1. Bacterial Strains and Culture

R. solanacearum cells were frozen at 75 °C in glycerol. For experimental use, *R. solanacearum* strains were cultured in NB medium (3.0 g/L beef extract, 1.0 g/L yeast extract, 5.0 g/L peptone and 10.0 g/L glucose, pH 7.0) in a humidified incubator overnight at 30 °C under constant agitation and then harvested at mid-exponential phase. After three washes in deionized water, the bacteria were resuspended in deionized water and diluted to 107–108 colony-forming units (CFU/mL) for experimental use.

2.2. Preparation of GO Suspensions

GO was prepared from natural graphite powders using modified Hummers method.[19] Briefly, the natural graphite powders (99.99%; Sigma-Aldrich) were initially oxidized using concentrated sulfuric acid (H_2SO_4) to produce graphite oxide (GtO). After being filtered and then washed with deionized water to remove chemical residues, the GtO was dispersed in deionized water and bath sonicated (Elamsonic, S60H) for 3 h to exfoliate and obtain a GO mixture.

2.3. Determination of Antibacterial Activity

To assess the antibacterial activity of GO towards bacterial cells, the prepared bacterial suspension was diluted with deionized water to obtain an initial optical density value of approximately 0.2 at 600 nm (OD600). Then, 100 μL aliquots of the cell suspension (107–108 CFU/mL) were injected into microcentrifuge tubes containing100 μL of different concentrations of the GO dispersion (125, 250, 500, and 1000 mg/L) for final GO concentrations of 62.5, 125, 250, and 500 mg/L. Following this, all of the samples were incubated for 2 h at 30 °C with gentle shaking. A mixture of the bacterial suspension and deionized water was used as a control. To determine the dependence of GO's activities on time and rotator speed, bacterial suspensions with 125 mg/L GO were incubated for 1 h, 2 h, 3 h and 4 h at 200 rpm and for 2 h at 100, 150, 200 and

250 rpm. Next, each sample was transferred into a 5 mL tube supplemented with 2 mL sterile NB medium, which was then fastened to an electronic oscillator and subjected to rotation at 250 rpm for 24 h at 30 °C. Bacterial growth was determined by measuring OD600 values at one-hour intervals. The OD600 values were recorded using a Nicolet Evolution 300 UV-Vis spectrometer.

To investigate the bactericidal activity of GO, exponentially growing *R. solanacearum* cells were harvested at an OD600 of 0.2 and washed twice with deionized water. Subsequently, the bacteria were mixed with the GO dispersions and incubated for 2 h at 120 rpm, after which 50 μL aliquots of serial 106-fold dilutions of the suspension were spread onto TZC agar (nutrient agar supplemented with 0.05% tetrazolium chloride) and allowed to grow for 2 days at 30 °C. The resultant colonies we recounted and used to calculate bacterial cell viability via comparisons against control plates. All treatments were repeated on at least three separate occasions. The cell death rate (% of control) was expressed using the following ratio: (counts of control—counts of treated samples)/counts of control. Using the above method, the cell viability of the bacteria exposed to GO for different periods of time (1 h, 2 h, 3 h, 4 h) and at varying rotator speeds (100, 150, 200, 250 rpm) was also investigated.

2.4. Outer Membrane Destabilization Assays

Exponentially growing *R. Solanacearum* cells were collected and thoroughly cleared by centrifugation before being suspended in 50 mM sodium HEPES buffer (pH 7.0) containing 5 mM glucose to obtain a concentration corresponding to an OD600 value of 0.2. Next, the bacteria were incubated with different concentrations of GO at room temperature for 5 min. The mixtures were washed and centrifuged at least three times to remove any remaining culture medium, and the resultant pellets were resuspended in HEPES buffer (pH 7.0) containing 5 mM glucose. SDS was added to the suspensions at a final concentration of 0.1%, and the OD600 was measured every two minutes thereafter.

2.5. ATP Assays

To determine total ATP levels in the bacterial cultures, exponentially growing *R. solanacearum* cells were collected and suspended in 50 mM sodium HEPES buffer (pH 7.0) containing 5 mM glucose to obtain an OD600 value of 0.1. After treatment with various concentrations of GO at room temperature, ATP was extracted with 1% trichloroacetic acid (TCA) in the presence of 2 mM EDTA. After incubation on ice for 30 min, the samples were neutralized with 2 volumes of 0.1 M Tris acetate (pH 7.8) to eliminate TCA interference. Then, the bacterial cultures were centrifuged, and the ATP levels in the supernatants were determined using an ATP assaykit obtained from Beyotime Biological Co., Ltd. (Beyotime, China).

2.6. Lipid Oxidation Measurement

The free radical modulation activity of graphene nanosheets was determined using a Lipid Peroxidation (MDA) Assay Kit (Sigma-Aldrich). In this kit, malondialdehyde (MDA) serves asan indicator of lipid peroxidation, which is measured via a reaction with thiobarbituric acid (TBA) to form a colored complex that can be measured using spectrofluorometric analysis. The level of MDA was presented as nmol mg^{-1} protein.

2.7. Protein Determination

The total protein in the *R. solanacearum* cells was measured using a BCA Protein Assay Kit (Beyotime Biological Co., Ltd., China) as previously detailed by Lowry et al.[21] Bovine serum albumin was used as a standard.

2.8. RNA Extraction and RT-qPCR Analysis of Gene Expression

Total cellular RNA was extracted using TRIzol reagent. Briefly, *R. solanacearum* cells were collected at the logarithmic phase and treated with GO at 250 μg/mL for 2 h. This GO concentration was chosen based on bactericidal activity assay results, which are presented in Figure 1. A control sample was treated with DI water. The cells were then centrifuged at 10,000 rpm for 10 min at 4 °C. A 100-μL aliquot of lysozyme was then immediately added to the cells and mixed. Following this, 1 mL TRIzol (Invitrogen, USA) was added to the mixture and left to sit for 5 minute, after which 0.2 ml of chloroform was layered into the tube. The mixture was then centrifuged at 10,000 rpm for 10 min at 4 °C. Next, the colorless upper aqueous phase was transferred into a clean, RNase-free tube, and 0.5 mL isopropanol was gently added at room temperature for RNA precipitation. The supernatant was then removed, and the RNA was washed twice with cold ethanol and dried. Finally, the obtained RNA was resuspended in ddH2O.

After purification, to eliminate DNA fragments, the RNA samples were subjected to DNase I treatment and reverse transcription (RT) as previously described. A 2-μL aliquot of the RNA was used as a template for cDNA synthesis, which was achieved using an iScript™ cDNA synthesis kit (Bio-Rad, USA) and a Bio-Rad real-time PCR system. After determining the concentration of the cDNA, quantitative PCR was performed using aone-step RT-qPCR kit. All primers were designed using Primer3 software and synthesized by the Beijing Genomics Institute. The primers were based on the *R. solanacearum* GMI1000 sequence, and their sequences are listed in Table I. RT-qPCR was performed using a 20 μL final reaction volume, which included 1 μL cDNA template, 7 μL RNase-free water, 7 μL Power SsoFast™ EvaGreen® supermix (Bio-Radlaboratories, USA), and 1 μL of each forward and reverse primer, in aCFX96TM Real-Time System (Bio-Rad, Hercules, CA, USA). The PCR amplification

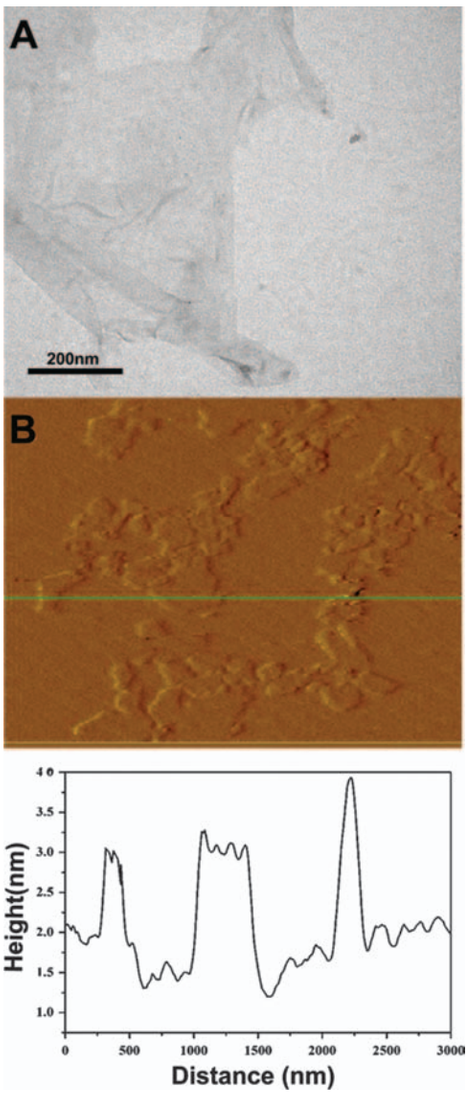

Figure 1. (A) TEM observations and (B) AFM images of GO sheets and their corresponding height profiles. GO was used at a concentration of 100 mg/mL for observation.

parameters included an initial denaturation at 95 °C for 3 min, a cycle of 95 °C for 10 s and 54 °C for 20 s, and 40 cycles of 60 °C for 30 s and 95 °C for 1 min. The relative RNA expression of each gene was quantitatively analyzed using CFX manager software, version 1.6 (Bio-Rad, USA). An endogenous gene (16sRNA) was used as a reference gene to validate the amplification efficiency of each primer. RNA with no reverse transcriptase was used as an additional control to eliminate the possibility of genomic DNA contamination. All treatments were analyzed in triplicate, including the qPCR analysis of each sample. Data analysis was performed using the $2_{T}^{\Delta\Delta-C}$ method, where $\Delta\Delta CT = \Delta CT(\text{treated sample}) - \Delta CT(\text{untreated sample})$, $\Delta CT = CT(\text{targetgene}) - CT(16S\ rRNA)$, and CT is the threshold cycle value for the amplified gene.[22]

2.9. Calculations and Statistical Analysis

All experiments were independently performed in triplicate. The results are expressed as the mean ± SD (standard deviation), and between-group comparisons were performed by analysis of variance (ANOVA) using Statistical Product and Service Solutions software (SPSS 11.0, United States). When assessing differences, the results were considered statistically significant when the P value was <0.05 or <0.01.

3. RESULTS AND DISCUSSION

3.1. Characterization of GO

In the current study, GO was synthesized by oxidizing natural graphite powders according to a modification of the classical Hummers method.[19] TEM was used to investigate the morphological structure of GO (Fig. 1). As seen in Figure 1(A), a representative TEM image of an exfoliated GO suspension at 100 mg/mL displayed a typical thin film and flat-sheet structure. In Figure 1(B), the exfoliated GO suspension is shown to have an average thickness of 0.634 nm, indicating that the GO sheets were successfully prepared.

3.2. Inhibition of Bacterial Growth

Bacterial growth measurement has been widely used to assess the antibacterial activities of nanomaterials. For a comprehensive understanding of how GO affects *R. solanacearum* growth, we quantified the growth of *R. solanacearum* cells by constructing a growth curve based on OD values obtained after cell incubation with various concentrations of GO for different lengths of time and at different rotator speeds. Considering that indirect interactions between GO and bacterial cells result incell membrane instability and membrane damage, the inhibitory effect of GO sheets on cell reproduction was remarkable. As shown in Figure 2(A), all of the tested GO concentrations (ranging from 62.5 to 500 μg/mL) led to growth suppression in less than 2 h of incubation time, retarding bacterial growth to the logarithmic phase. The bacteriostatic activity of GO increased as its concentration increased. Moreover, incubation time and rotation speed also had an extreme influence on the antibacterial behavior of GO. In the presence of 125 μg/mL GO, bacteria cell reproduction became restrained within 1 h. Similarly, bacteria incubated with a lower dose of GO (125 μg/mL) at a rotation speed of 150–200 rpm showed statistically significant decreases in cell proliferation.

3.3. Bactericidal Effect of GO Against *R. solanacearum*

The bactericidal effect of GO on *R. solanacearum* proliferation was investigated under various treatment conditions. *R. solanacearum* cells were collected during the logarithmic phase (107–108 CFU/mL) and incubated with different concentrations (62.5, 125, 250, and 500 μg/mL) of

Table I. Primers sequence of genes selected for RT-qPCR.

Gene	Function or protein encoded	Primer	Sequence (5′–3′)
Virulence genes			
phcA	Virulence transcription regulator protein	Forward	TTGTAGGTCTCGCACACCAG
		Reverse	GCTCGCTCGATCAGTACCTC
vsrC	Response regulator, transcription regulator protein	Forward	ACCACCCTCTCGCCTTATCT
		Reverse	ACAGCCAGACATCCAGCAG
xpsR	Transcription regulator	Forward	AGATCGACATAGCGCTGCTT
		Reverse	TTACTTTGCGGACCTGCTCT
epsE	EPS I polysaccharide export inner membrane protein	Forward	CTGGATAAAGCCACGCAAAG
		Reverse	CAGTGGTACATCGCCATCAC
prhG	Transcription response regulator	Forward	TCCAGATGCTGATGATCGAC
		Reverse	AGTTCGTCCGCAGAGAAATG
pehC	Polygalacturonase	Forward	CTCAGCAACGTCAACTTCCA
		Reverse	CCGTAGTTCAGGCAATCGTT
solR	Transcriptional activator transcription regulator protein	Forward	GCTCGGCTTTGACTACTGCT
		Reverse	CCTCATCACGGATGGACAC
hrpB	Transcriptional activator of hrp genes cluster; type III secretion system protein	Forward	AATACGCAAATGCGGTTTTC
		Reverse	CTTCTTCCGCTTCTTCATCG
popA	Type III secretion system and secreted effector proteins	Forward	AACCAGGATCCGATGCAAGC
		Reverse	GCTTCACCAGGTCTTCCAGC
Oxidative stress genes			
oxyR	Hydrogenperoxide-induciblegenes activator transcription regulator protein	Forward	ACCAGCCGCGCGGTGAAGTTT
		Reverse	ACGATCGGGCCGTACCTGCT
sodB	Probable superoxide dismutase [fe] protein	Forward	TCACGAACCTGAACAACCTG
		Reverse	GCGACCTTGGTGAACTCTTC
ahpC	Putative alkyl hydroperoxide reductase (subunitc) oxidoreductase protein	Forward	CGAGGTCTACATCGTCACCA
		Reverse	GGTCTTGATCACGCCTTCC
dps	Oxidativetress transcription regulator protein	Forward	GGACCGCCGTGGATTCGGTGG
		Reverse	CCGGGAACAGGCTGCGTGCG
Mobility genes			
ohrB	Organic hydroperoxide resistance protein	Forward	GCTCATGGATACACGCAAGA
		Reverse	AGCACCAGCATCACCAAGTA
pilT	Fimbrial type-4 assembly membrane transmembrane protein	Forward	GGTACCTCTAGACATCGTGGC
		Reverse	ACTCCGGAGC GGTACCTCTAGACATCGTGGC ACTCCGGAGC
egl	Endoglucanase precursor (Endo-1,4-beta-glucanase) (Cellulase)	Forward	AAATCCAGATATCGAATTGCCAA
		Reverse	GCGTGCCGTACCAGTTCTG
filA	Pilus subunit	Forward	TTCGTAGTACAGCAGTTGGCT
		Reverse	GCAGTTCGAGTTCTATGCCG
flgM	Negative regulator of flagellin synthesis (anti-sigma-28 factor) protein	Forward	GGCCATCACGCCGACCAA
		Reverse	GCGAGACCTGCTGCACCGA
Reference genes			
rplM	50S ribosomal protein	Forward	CCGCAAAGCCCCATGAG
		Reverse	TGTCCGTCGCGTCAATCA
16S rRNA	16S rRNA	Forward	AGAGTTTGATCCTGGCTCAG
		Reverse	ACGGCTACCTTGTTA

GO for 2 hat a rotator speed of 200 rpm. After spreading the bacterial suspensions on TZC agar and allowing them to grow, bacterial viability was determined using a colony counting method. A control sample that was treated with DI water was included. As shown in Figure 3(A), as the GO concentration increased, a gradual increase in cellular toxicity was observed, with cell viability percentages of 38.7%, 34.1%, 16.4% and 13.4% following GO treatment, in comparison with 97.36% following the control treatment. Additionally, incubation time and rotation speed significantly affected the death rate of *R. solanacearum*. In the above experiment, GO was shown to possess time-dependent and speed-dependent antibacterial actions. Following incubation with 125 μg/mL GO for 1 h, the cell survival rate was 82.21%; after incubation for 4 h, this rate decreased to 23.4%, a difference of 3.5-fold. We selected

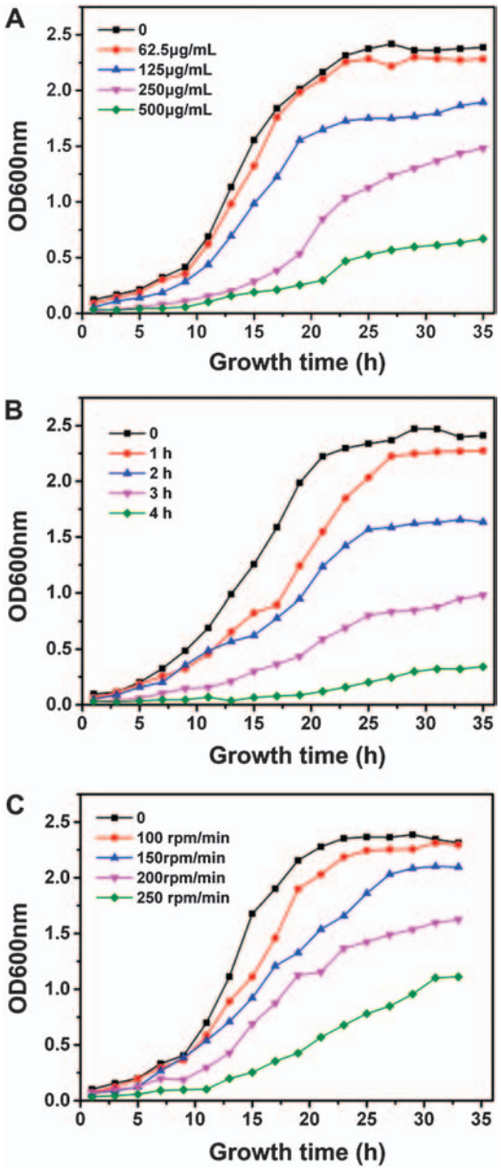

Figure 2. Growth of *R. solanacearum* cells following exposure to different concentrations of GO for 2 h (A), to 125 μg/mL GO for different lengths of time at 200 rpm, and (C) to 125 μg/mL GO for 2 h at different rotation speeds.

this moderate concentration to assess the effects of rotator speed on GO-induced toxicity. After incubation with 125 μg/mL GO for 2 h, a gradual decrease in bacterial viability was observed as the rotator speed increased from 50 rpm to 200 rpm, reaching significance at 100 rpm. At 200 rpm, the bacterial viability was 23.01%, compared to 98.4% in the control sample.

3.4. Cellular Membrane Destabilization

R. solanacearum, a Gram-negative, pathogenic bacterium, possesses two membrane layers, which serve as an effective barrier to resist various noxious agents, macromolecules and the majority of hydrophobic substances,[23] especially the outer membrane. Additionally, the membrane surface is decorated with polyanionic lipopolysaccharide (LPS), enabling it to bind to cationic molecules, which are essential for the integrity of the cytoplasmic membrane. Membrane integrity can be affected by physical and chemical damage, such as freezing temperatures, heat, and UV irradiation.[24] In some cases, outer membrane permeability changes as a result of its susceptibility to the bacteriolytic actions of detergents and lysozyme.[25, 26] Therefore, we evaluated the effect of GO in terms of outer membrane destabilization and integrity by measuring sensitization to sodium dodecyl sulfate (SDS), which possesses bacteriolytic action. *R. solanacearum* cells were treated with GO, washed to remove excess material, and quantified via the determination of OD600 value. As shown in Figure 4(A), bacteria that were incubated with various concentrations of GO exhibited increased susceptibility to the bacteriolytic action of SDS, as shown by a substantial reduction in OD600 value; these effects were GO concentration-dependent.

Meanwhile, the effects of GO sheets on cytoplasmic membrane integrity in *R. solanacearum* were surveyed by TEM. TEM enabled us to not only observe cell membrane integrity but also to assess changes in cell morphology in the presence of GO. Despite a previous study claiming that bacterial contact with the edges of GO sheets is not a fundamental aspect of GO's antibacterial mechanism,[27] we found that bacterial cell membranes became fuzzy in appearance (blank arrows) after coming into contact with GO, unlike untreated bacteria, which maintained completely intact and distinct membrane structures (Fig. 4(B)). Based on the results of the above analyses, it seems in conceivable to us that the bacteria cell membrane remains stable after exposure to GO. These results were in agreement with a previous study by Akhavan et al.[28] In previous publications, both direct and indirect interactions between nanomaterials and biological cells have been demonstrated.[29] Based on its physical and chemical properties, GO exhibited essentially toxicity toward microbes, including bacteria and fungi. GO's effects on cell morphology are expected to be a significant factor in its antibacterial activity. As shown in this study, GO treatment resulted in membrane damage, which was characterized by a number of additional events, including nucleic acid leakage and changes in membrane potential. We assessed the sensitivity of cell membrane permeability as an indicator to evaluate the effect of GO on *R. solanacearum* cells and found that cell membranes were disturbed in the presence of GO (Fig. 4). These results are concordant with previous studies.[8, 11]

3.5. ATP Level Analysis

Biomolecules, including some proteins, are imported into cells through the cytoplasmic membrane, which requires

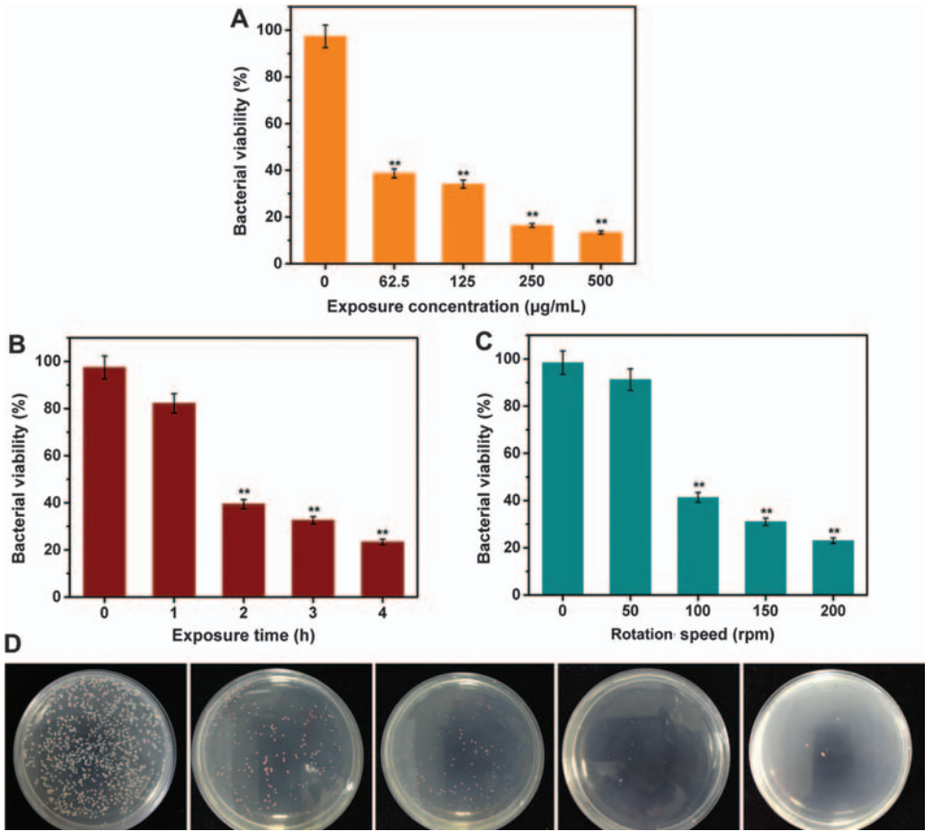

Figure 3. (A) Viability of *R. solanacearum* cells after treatment with different concentrations of GO for 2 h at 30 °C, (B) after incubation with 125 μg/mL GO for different lengths of time at 200 rpm, and (C) after incubation with 125 μg/mL GO for 2 hat different rotation speeds. (D) Images of *R. solanacearum* colonies on agar plates after treatment with different concentrations of GO (0, 62.5, 125, 250 and 500 μg/mL).

energy produced by physiological metabolic activity. GO sheets can come into contact and intertwine with bacteria cells by covering their surfaces.[11] It has been proposed that electrostatic attraction improves the adhesion of charged nanoparticles to cell membranes.[30] Therefore, we inferred that GO disturbs microbial cell membranes while simultaneously disturbing normal ATP production, primarily by affecting vital membrane-associated energy-transducing enzymes.[31] From our results, it is obvious that treatment with GO at a high concentration led to a gradual reduction in ATP level in *R. solanacearum* over the experimental time course, eventually leading to the virtual absence of ATP. It has also been reported that some metal nanoparticles, such as silver nanoparticles, can deplete the ATP content of bacterial cells within 5 min, with no evidence of ATP leakage.[32]

3.6. Lipid Peroxidation

In general, the toxicity against biological samples induced by nanoparticles has been largely attributed to physical damage or chemical stress.[33,34] Carbon-based nanomaterials, such as CNTs and fullerene, have been proven to induce oxidative stress in cells and bacteria, which is mediated by derived free radicals.[35] In the case of GO, previous studies have suggested that ROS production underlies its toxicity.[8] Beyond that, it is well-known that lipid peroxidation in the liposomal membrane generally occurs through a process in which oxidants such as free radicals attack lipids containing carbon–carbon double bond(s), especially polyunsaturated fatty acids (PUFAs).[36] To evaluate the effects of GO on bacterial energy-transducing processes and metabolism, it is necessary to measure the oxidative stress response. As shown in Figure 7, in comparison with untreated cells, we observed that MDA content in *R. solanacearum* increased by 229% and 347% after incubation with 250 and 500 μg/mL of GO, respectively, indicating the stimulation of lipid peroxidation. This increase in lipid peroxidation after GO exposure may be attributed to the induction of ROS, such as reactive hydroxyl radicals and singlet oxygen molecules, which enhance the oxidation of polyunsaturated fatty acids and result in lipid peroxidation.[18] Lipid peroxidation in biological cells can result in modification of and damage to nucleic acids and membrane proteins, potentially causing cell membrane disintegration and cell death. These results were in agreement with a previous study by Liu et al.[8]

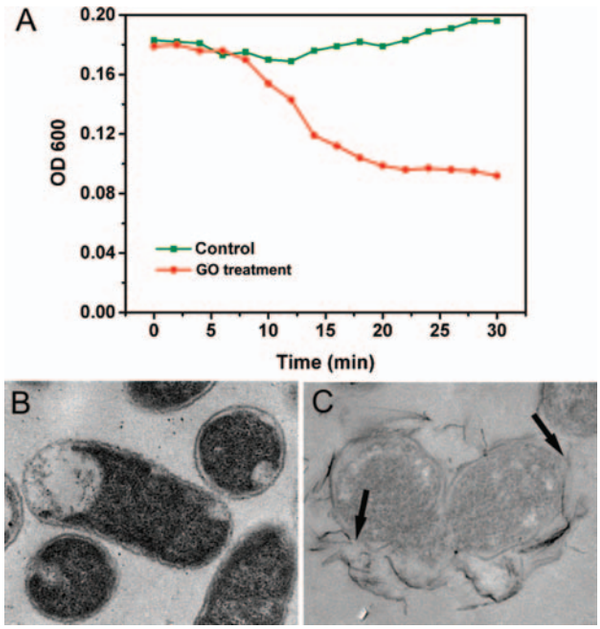

Figure 4. (A) Effects of GO treatment on *R. solanacearum* cell membranes. (B) *R. solanacearum* cell membrane morphology after incubation with sterile water without GO sheets and with 500 μg/mL GO sheets (C) for 2 h at 30 °C. The images were taken at 8000× magnification.

3.7. Gene Expression Profile in *R. solanacearum* After Go Treatment

Transcriptomic and proteomic analyses have been widely used in studying the molecular mechanisms underlying the actions of antibacterial agents. To elucidate the molecular mechanism driving the antibacterial activity of GO sheets against *R. solanacearum*, in this experiment, we investigated the expression of several genes related to motility, oxidative stress and virulence after treatment with a 500 μg/mL GO suspension for 30 min. Gene expression

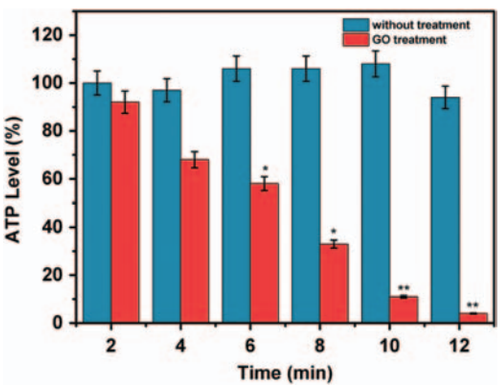

Figure 5. ATP contentin GO-treated and untreated bacteria. Exponentially growing *R. solanacearum* cells were suspended in HEPES buffer containing 50 mM sodium and 5 mM glucose (pH 7.0) to an OD600 of 0.2 and then treated with GO at varying concentrations (0, 62.5, 125, 250 and 500 μg/mL) at room temperature. ATP levels were determined at timed intervals. The ATP level in the untreated bacterial culture was 3.6 nmol/mg cell protein, which was considered 100%.

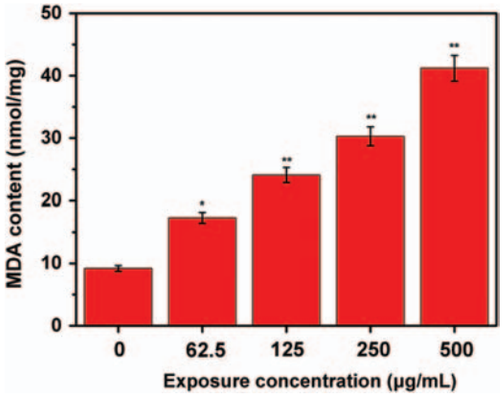

Figure 6. MDA content in *R. solanacearum* cells in the presence of different concentrations of GO. MDA level was used as an indicator of lipid peroxidation.

was quantified by RT-qPCR. As shown in Figure 7, the expression levels of all of the selected virulence genes (*phcA*, *vsrC*, *xpsR*, *epsE*, *pehC*, *solR* and *hrpB*) were downregulated in bacteria, with the exception of *popA* expression, which did not appear to change. In particular, *phcA* and *hrpB* were significantly down regulated, by 2.61- and 3.45-fold compared to the control. Conversely, the expression levels of several important oxidative stress genes were upregulated in the GO-treated sample: *sodB*, *oxyR* and *dps* expression increased by 1.82-, 2.17-, and 3.79-fold, respectively. The expression levels of all assessed genes related to bacterial mobility decreased.

R. solanacearum virulence is determined by a complex network of factors, including contributions from the Type III secretion system (TTSS), the Type II secretion

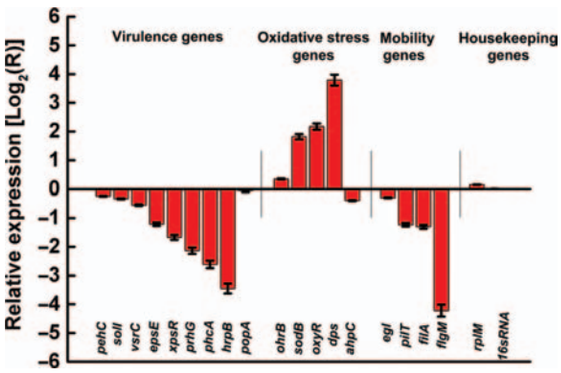

Figure 7. Relative gene expression levels in GO-treated and untreated *R. solanacearum* cells. The cells were collected during the logarithmic growth phase. After incubation with 125 μg/ml GO for 2 h, the expression levels of the indicated genes were quantified by RT-qPCR. Relative gene expression levels were analyzed using a comparative critical threshold method. Compared with untreated sample, the relative expression ratio for each gene is presented as a $\log_2$ value in the histogram. A ratio greater than zero indicates upregulation of gene expression, and a ratio below zero indicates downregulation. *rpmM* and 16 sRNA were used as reference genes to ensure the amplification efficiency of each primer. The vertical bar represents the standard deviation of three replicates.

system, extracellular polysaccharides and several plant cell wall-degrading enzymes.[12, 37–39] Few studies have focused on the antibacterial mechanism of GO at the molecular level. However, other carbon-based nanomaterials, such as SWCNT, have previously been shown to exclusively downregulate several major virulence genes in *Salmonella typhimurium*.[40] In the current study, results from evaluating gene transcription confirmed that GO down regulates the expression of genes related to pathogenicity in *R. solanacearum*, including *Hrp* and *PhcA* (Fig. 8). Both of these genes play vital roles in regulating pathogenesis. *HrpB*, a *Hrp* gene family member encoding Type III secretion machinery, isa crucial transcriptional activator involved in *R. solanacearum* pathogenicity.[12] This gene has been shown to control infection, vascular colonization and multiplication of *R. solanacearum* in plants.[41] *PhcA* is a member of the *LysR* family of transcriptional regulators, which is considered a central element of this intricate system.[42] Although the *popA* gene, a type III effector, was virtually unaffected by GO, this gene has been proven to not be essential for *R. solanacearum* pathogenicity.[43] Based on the gene expression profile produced using RT-PCR, GO is likely to reduce virulence after forming direct interactions with bacterial cells.

Microorganisms, including bacteria and fungi, can mediate or resist damage induced by fluctuations in their immediate surroundings by utilizing their various stress response systems, which can protect from injury and increase survival.[44] In bacteria, these stress responses involve a complex network of elements, the most important of which regulate gene expression and defensive protein activity.[45] Commonly, pathogenic bacteria utilize transcription-based defensive regulatory systems when exposed to oxidative stress: Gene expression profiles are re-programmed, particularly those corresponding to proteins involved in signal transduction and regulation, ROS-scavenging, and oxidative damage repair; this process is termed the oxidative stress response (OSR).[46] In the current paper, our results indicated that increased lipid peroxidation was triggered in *R. solanacearum* in the presence of GO (Fig. 6). Additionally, RT-qPCR measurement revealed that, during exposure to stress, the expression levels of a series of oxidative defense genes (*ohrB*, *sodB*, *oxyR*, *dps*) were upregulated. *OxyR* is dox-sensing *LysR* family transcriptional regulator that has been reported to both activate and repress the transcription of target genes in other bacterial species.[47, 48] GO-induced hydrogen peroxide production in *R. solanacearum* led to increased expression of *aphC*, which is typically expressed in an OxyR-dependent manner.[49] Another nonspecific DNA-binding protein encoded by the *dps* gene was also upregulated by the oxidative stress response regulator OxyR.[50] It can be concluded that the induction of oxidative stress in *R. solanacearum* by GO may be a significant component of its antibacterial mechanism, which is similar to observations made in *Campylobacter* and *C. jejuni* after exposure to ZnO nanoparticles.[45] Many studies have demonstrated that GO treatment induces ROS production in bacteria cells, which can cause severe macromolecular damage, leading to mutations and cell death.[8] Other studies have found that CNTs upregulate the expression of genes related to stress response, the *soxRS* and *oxyR* systems, glycolysis, fatty acid beta-oxidation, and fatty acid biosynthesis pathways.[51, 52] Stress-response proteins are considered "effective scavengers" and serve to eliminate ROS species (e.g., H_2O_2, O^{-2}) while simultaneously attempting to repair molecules damaged by oxidation.[46] Although cells are able to activate robust defensive systems, ROS production still causes damage by causing alterations in macromolecules, such as polyunsaturated fatty acids in membrane lipids; protein denaturation; and ultimately DNA damage.[53] These processes lead to cell growth inhibition and cell death, which was observed in our experiments. As show in Figure 6, lipid peroxidation significantly increased following GO exposure, and cell membranes were injured; these effects were both significant factors that led to bacterial cell death (Fig. 3).

We also analyzed the effects of GO on the expression of mobility genes, another component of virulence, and found that GO repressed the expression of four mobility-related genes. It is well known that flagella-driven swimming motility of *R. solanacearum* contributes significantly to its invasion of and therefore virulence towards plants.[54] This observation was confirmed by the fact that GO induced a remarkable reduction in the virulence of *R. solanacearum*. Based on the presented results, there appear to be two key components underlying GO's interactions with bacteria: First, the nanoparticles attach to the bacterial cell surface, damaging membrane structures and subsequently affecting energy metabolism and lipid peroxidation. Second, and perhaps more importantly, GO downregulates the expression of several genes associated with virulence towards plants.

4. CONCLUSIONS

In conclusion, we investigated the antibacterial activity of GO toward the phytopathogen *R. solanacearum* and discussed its effects on bacterial energy metabolism and the mechanisms underlying its toxicity at the molecular level. To the best of our knowledge, this is the first report of GO-induced toxicity and the associated underlying mechanisms. GO was found to exhibit concentration-, exposure time- and rotation speed-dependent bacteriostatic and bactericidal activities. Additionally, exposure to GO significantly destabilized bacterial cell membranes. Cellular ATP levels gradually declined as a result of increasing GO concentrations. Furthermore, GO-treated bacteria exhibited enhanced lipid oxidation. RT-qPCR analysis indicated that GO significantly downregulated the expression of genes related to virulence and motility in *R. solanacearum*, while important oxidative stress-response genes (*sodB*, *oxyR* and

dps) were upregulated. Our observations on GO-induced toxicity in *R. solanacearum* suggest that the possible mechanism underlying GO's activities is cell membrane injury, leading to membrane destabilization, disturbing essential energy metabolism and inducing oxidative stress.

Acknowledgments: This work was financially supported through grants from the Fundamental Research Funds for the Central Universities (2120132349), the National Natural Science Foundation of China (31272058), the Key Project of the State Tobacco Monopoly Administration (NY20130501070005) and the Key Project of the Chongqing Tobacco Monopoly Administration (110201202002).

References and Notes

1. L. R. Khot, S. Sankaran, J. M. Maja, R. Ehsani, and E. W. Schuster, *Crop Prot.* 35, 64 (**2012**).
2. V. Ghormade, M. V. Deshpande, and K. M. Paknikar, *Biotechnology Adv.* 29, 792 (**2011**).
3. O. C. Compton and S. T. Nguyen, *Small* 6, 711 (**2010**).
4. A. K. Geim, *Science* 324, 1530 (**2009**).
5. S. Singh and H. S. Nalwa, *J. Nanosci. Nanotechnol.* 7, 3048 (**2007**).
6. W. Hu, C. Peng, W. Luo, M. Lv, X. Li, D. Li, Q. Huang, and C. Fan, *ACS Nano* 4, 4317 (**2010**).
7. G. Gonavelli, C.-C. Chang, and Y.-C. Ling, *ACS Sustain. Chem. Eng.* 1, 462 (**2013**).
8. S. Liu, T. H. Zeng, M. Hofmann, E. Burcombe, J. Wei, R. Jiang, J. Kong, and Y. Chen, *ACS Nano* 5, 6971 (**2011**).
9. J. Li, G. Wang, H. Zhu, M. Zhang, X. Zheng, Z. Di, X. Liu, and X. Wang, *Scientific Rep-UK* 4, 4359 (**2014**).
10. J. Chen, X. Wang, and H. Han, *J. Nanopart. Res.* 15, 1 (**2013**).
11. J. Chen, H. Peng, X. Wang, F. Shao, Z. Yuan, and H. Han, *Nanoscale* 6, 1879 (**2014**).
12. M. Salanoubat, S. Genin, F. Artiguenave, J. Gouzy, S. Mangenot, M. Arlat, A. Billault, P. Brottier, J. C. Camus, L. Cattolico, M. Chandler, N. Choisne, C. Claudel-Renard, S. Cunnac, N. Demange, C. Gaspin, M. Lavie, A. Moisan, C. Robert, W. Saurin, T. Schiex, P. Siguier, P. Thebault, M. Whalen, P. Wincker, M. Levy, J. Weissenbach, and C. A. Boucher, *Nature* 415, 497 (**2002**).
13. A. C. Hayward, *Annual Rev. Phytopathol.* 29, 65 (**1991**).
14. J. Vasse, P. Frey, and A. Trigalet, *Mol. Plant-Microbe In.* 8, 241 (**1995**).
15. S. Seo, K. Gomi, H. Kaku, H. Abe, H. Seto, S. Nakatsu, M. Neya, M. Kobayashi, K. Nakaho, Y. Ichinose, I. Mitsuhara, and Y. Ohashi, *Plant Cell Physiol.* 53, 1432 (**2012**).
16. Y. Tu, M. Lv, P. Xiu, H. Tien, M. Zhang, M. Castelli, Z. Liu, Q. Huang, C. Fan, H. Fang, and R. Zhou, *Nat. Nanotechnol.* 8, 594 (**2013**).
17. M. Hans, A. Erbe, S. Mathews, Y. Chen, M. Solioz, and F. Muecklich, *Langmuir* 29, 16160 (**2013**).
18. A. Valavanidis, T. Vlahogianni, M. Dassenakis, and M. Scoullos, *Ecotox. Environ. Safe.* 64, 178 (**2006**).
19. W. S. Hummers and R. E. Offeman, *J. Am. Chem. Soc.* 80, 1339 (**1958**).
20. A. Kelman, *Phytopathology* 44, 693 (**1954**).
21. O. H. Lowry, N. J. Rosebrough, A. L. Farr, and R. J. Randall, *J. Biolo. Chem.* 193, 265 (**1951**).
22. T. D. Schmittgen and K. J. Livak, *Nat. Protoc.* 3, 1101 (**2008**).
23. Jw. Costerto, J. M. Ingram, and K. J. Cheng, *Bacteriol. Rev.* 38, 87 (**1974**).
24. A. M. Wesche, J. B. Gurtler, B. P. Marks, and E. T. Ryser, *J. Food Protect.* 72, 1121 (**2009**).
25. H. L. Alakomi, E. Skytta, M. Saarela, T. Mattila-Sandholm, K. Latva-Kala, and I. M. Helander, *Appl. Environ. Microb.* 66, 2001 (**2000**).
26. M. Vaara, *Microbiol. Rev.* 56, 395 (**1992**).
27. J. D. Mangadlao, C. M. Santos, M. J. L. Felipe, A. C. C. de Leon, D. F. Rodrigues, and R. C. Advincula, *Chem. Commun.* 51, 2886 (**2015**).
28. O. Akhavan, E. Ghaderi, and A. Esfandiar, *J. Phys. Chem. B* 115, 6279 (**2011**).
29. Y. L. Zhao and H. S. Nalwa, (eds.), Nanotoxicology-Interactions of Nanomaterials with Biological Systems, American Scientific Publishers, Los Angeles, CA (**2007**).
30. Y. Li and N. Gu, *J. Phys. Chem. B* 114, 2749 (**2010**).
31. T. J. Bradley, Membranes as Sites of Energy Transduction (**2009**).
32. C. N. Lok, C. M. Ho, R. Chen, Q. Y. He, W. Y. Yu, H. Z. Sun, P. K. H. Tam, J. F. Chiu, and C. M. Che, *J. Proteome Res.* 5, 916 (**2006**).
33. T. Xia, M. Kovochich, J. Brant, M. Hotze, J. Sempf, T. Oberley, C. Sioutas, J. I. Yeh, M. R. Wiesner, and A. E. Nel, *Nano Lett.* 6, 1794 (**2006**).
34. G. Bhabra, A. Sood, B. Fisher, L. Cartwright, M. Saunders, W. H. Evans, A. Surprenant, G. Lopez-Castejon, S. Mann, S. A. Davis, L. A. Hails, E. Ingham, P. Verkade, J. Lane, K. Heesom, R. Newson, and C. P. Case, *Nat. Nanotechnol.* 4, 876 (**2009**).
35. S. Kang, M. S. Mauter, and M. Elimelech, *Environ. Sci. Technol* 43, 2648 (**2009**).
36. S. N. Chatterjee and S. Agarwal, *Free Radical Biol. Med.* 4, 51 (**1988**).
37. E. T. Gonzalez and C. Allen, *Mol. Plant Microbe In.* 16, 536 (**2003**).
38. E. Saile, J. A. McGarvey, M. A. Schell, and T. P. Denny, *Phytopathology* 87, 1264 (**1997**).
39. M. A. Schell, *Annu. Rev. Phytopathol.* 38, 263 (**2000**).
40. A. A. Chaudhari, S. L. Jasper, E. Dosunmu, M. E. Miller, R. D. Arnold, S. R. Singh, and S. Pillai, *J. Nanobiotechnol.* 13, 23 (**2015**).
41. J. Vasse, S. Genin, P. Frey, C. Boucher, and B. Brito, *Mol. Plant Microbe In.* 13, 259 (**2000**).
42. S. J. Clough, A. B. Flavier, M. A. Schell, and T. P. Denny, *Appl. Environ. Microb.* 63, 844 (**1997**).
43. M. Arlat, F. Vangijsegem, J. C. Huet, J. C. Pernollet, and C. A. Boucher, *Embo J.* 13, 543 (**1994**).
44. K. J. Boor, *Plos Biol.* 4, 18 (**2006**).
45. Y. Xie, Y. He, P. L. Irwin, T. Jin, and X. Shi, *Appl. Environ. Microb.* 77, 2325 (**2011**).
46. A. Kaur, P. T. Van, C. R. Busch, C. K. Robinson, M. Pan, W. L. Pang, D. J. Reiss, J. DiRuggiero, and N. S. Baliga, *Mol. Syst. Biol.* 6, 393 (**2010**).
47. R. Ieva, D. Roncarati, M. M. E. Metruccio, K. L. Seib, V. Scarlato, and I. Delany, *Mol. Microbiol.* 70, 1152 (**2008**).
48. Y. J. Heo, I. Y. Chung, W. J. Cho, B. Y. Lee, J. H. Kim, K. H. Choi, J. W. Lee, D. J. Hassett, and Y. H. Cho, *J. Bacteriol.* 192, 381 (**2010**).
49. Z. Flores-Cruz and C. Allen, *Appl. Environ. Microb.* 77, 6426 (**2011**).
50. J. M. Colburn-Clifford, J. M. Scherf, and C. Allen, *Appl. Environ. Microb.* 76, 7392 (**2010**).
51. S. Kang, M. Herzberg, D. F. Rodrigues, and M. Elimelech, *Langmuir* 24, 6409 (**2008**).
52. S. Sarkar, C. Sharma, R. Yog, A. Periakaruppan, O. Jejelowo, R. Thomas, E. V. Barrera, A. C. Rice-Ficht, B. L. Wilson, and G. T. Ramesh, *J. Nanosci. Nanotechnol.* 7, 584 (**2007**).
53. V. C. Sanchez, A. Jachak, R. H. Hurt, and A. B. Kane, *Chem. Res. Toxicol.* 25, 15 (**2011**).
54. J. Tans-Kersten, H. Y. Huang, and C. Allen, *J. Bacteriol.* 183, 3597 (**2001**).

Received: 11 September 2015. Accepted: 29 October 2015.